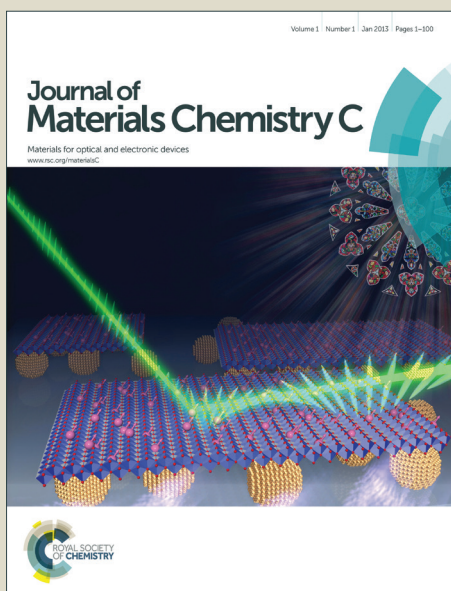


Journal of Materials Chemistry C

Accepted Manuscript



This is an *Accepted Manuscript*, which has been through the Royal Society of Chemistry peer review process and has been accepted for publication.

Accepted Manuscripts are published online shortly after acceptance, before technical editing, formatting and proof reading. Using this free service, authors can make their results available to the community, in citable form, before we publish the edited article. We will replace this *Accepted Manuscript* with the edited and formatted *Advance Article* as soon as it is available.

You can find more information about *Accepted Manuscripts* in the [Information for Authors](#).

Please note that technical editing may introduce minor changes to the text and/or graphics, which may alter content. The journal's standard [Terms & Conditions](#) and the [Ethical guidelines](#) still apply. In no event shall the Royal Society of Chemistry be held responsible for any errors or omissions in this *Accepted Manuscript* or any consequences arising from the use of any information it contains.

COMMUNICATION

Large-area nanoscale farmland-like surfaces of one-dimensional NbO₂ nanorods with multi-growth directions: Studies on the purple-blue photoluminescence and low-field electron emissions

Cite this: DOI: 10.1039/x0xx00000x

Received 00th January 2014,
Accepted 00th January 2014

DOI: 10.1039/x0xx00000x

www.rsc.org/

Jin-Han Lin,^{a,b} Ranjit A. Patil,^a Ming-Ann Wu,^a Lian-Guang Yu,^a Ken-Da Liu,^a Wan-Ting Gao,^a Rupesh S. Devan,^c Ching-Hwa Ho,^d Yung Liou,^b and Yuan-Ron Ma*^a

We synthesized a scenic morphological form of a large-area NbO₂ nanoscale farmland using the hot-filament metal-oxide vapor deposition technique (HFMOVD). The nanoscale farmland is comprised of one-dimensional (1D) NbO₂ nanorods arranged in various domains, which grow in multi-directions. However, each domain contains ~620 nanorods per square micrometer and has its own growth direction. The 1D NbO₂ nanorods are found to have purple-blue photoluminescence (PL) emissions at room-temperature as well as very low turn-on and threshold fields for field emission (FE). The PL and FE results indicate that the 1D NbO₂ nanorods are brilliant light and electron emitters.

A. Introduction

Metal oxides are some of the most fascinating functional materials, and one-dimensional (1D) metal-oxide nanostructures have recently attracted much attention. These 1D nanostructures have some unique properties, which make them suitable for a wide variety of applications,^[1] such as for light emitting diodes, electrochromic devices, supercapacitors, field emitters, gas sensors, nanoelectronics, and nanogenerators. Hence, a lot of effort has been made to synthesize and characterize 1D metal-oxide nanostructures in any possible shape. Niobium oxides contain stoichiometric NbO,^[2] NbO₂,^[3] Nb₂O₅,^[2,4-8] Nb₁₀O₂₅,^[9] and non-stoichiometric Nb₁₂O₂₉,^[10,11] and Nb₂₂O₅₄,^[9,11] all based only on a network of NbO₄ tetrahedrons and NbO₆ octahedrons with shared oxygen atoms.^[2] In addition, niobium oxides possess excellent physical properties, such as having a wide band gap^[12] and high refractive index,^[12,13] and they can be made in a variety of crystalline phases, including orthorhombic, tetragonal, monoclinic, cubic, and hexagonal. By varying the chemical compositions and crystalline phases, they can be tailored to make them useful for a variety of applications requiring catalysis,^[4] field emission,^[5] photovoltaic,^[6] and electrochromic effects.^[8] In the quest for a 1D morphology, many deposition methods have been developed. 1D niobium oxide nanostructures can be grown in the forms of nanowires,^[4,5,14-16] nanorods,^[8] nanobelts,^[6] nanotubes,^[17] nanoslices,^[3] and so on.

In this study, a scenic nanoscale farmland, consisting of high-density 1D NbO₂ nanorods arranged in various domains, is synthesized using hot-filament metal-oxide vapor deposition (HFMOVD) technique. The 1D NbO₂ nanorods grow in multi-growth directions in the scenic nanoscale farmland, but each

domain contains ~620 nanorods per square micrometer and has its own growth direction. This HFMOVD technique is very versatile, because it can be used to synthesize a wide range of metal-oxide^[18-29] and metal^[30-34] nanostructures with varying morphologies and crystalline traits. The photoluminescence (PL) light emissions at deep levels in the band gap were probed by PL spectroscopy. The room-temperature PL spectra showed a wide-range of emissions from ultraviolet (UV) to infrared (IR), but the PL emissions largely look purple-blue. The field emissions (FEs) of the high-density 1D NbO₂ nanorods were explored using an electrometer and a tantalum (Ta) ball-probe. The room-temperature FE graphs showed the 1D NbO₂ nanorods to be excellent electron emitters, because they have a very low turn-on field of 1.5 V/μm (at a current density of 11.2 μA/cm²) and a threshold field of 2.4 V/μm (at a current density of 1.1 mA/cm²). The PL and FE results strongly indicate that the 1D NbO₂ nanorods are good and effective light and electron emitters at room temperature, consequently confirming the feasibility of the scenic NbO₂ nanoscale farmland as a potential candidate for the fabrication of optoelectronic nanodevices and commercial flat displays.

B. Experimental details

The large-area nanoscale farmland-like surface, consisting of high-density 1D NbO₂ nanorods arranged in various domains, was synthesized utilizing the HFMOVD technique. Clean niobium (Nb) wires (99.8% pure) with a diameter of 1 mm were passed through a graphite disk and fixed to two supporting copper electrodes mounted

in a vacuum chamber. When the pressure of the vacuum chamber was pumped down to $\sim 1 \times 10^{-2}$ Torr, the Nb wires were heated to ~ 1750 °C for 20 minutes to generate hot niobium vapor. The niobium vapor met and reacted with the residual oxygen to form a metal-oxide vapor of NbO_x . The metal-oxide vapor condensed to form 1D NbO_2 nanorods on a silicon substrate (8×20 mm²) with a substrate temperature of ~ 450 °C. The 1D NbO_2 nanorods were examined by a field-emission scanning electron microscope (FESEM, JEOL JSM-6500F). The crystalline structures of the 1D NbO_2 nanorods were probed by an X-ray diffractometer (XRD, Rigaku D/max-2500) equipped with Cu K α radiation ($\lambda = 1.541$ Å). The PL properties of the 1D NbO_2 nanorods were studied by a spectrometer (Ocean Optics, QE65000) equipped with a CCD detector array. The pumping light source was a 325 nm He-Cd laser filtered by a long-pass filter with a cutting edge of 340 nm for shielding the plasma lines. Field emission measurements were performed with an electrometer (Keithley 2410) in a vacuum chamber at a pressure of 2×10^{-7} Torr. A Ta ball-probe with a radius ($\equiv r$) of ~ 750 μm , used as the anodic electrode, was 50 μm away from the 1D NbO_2 nanorods (cathode). Direct-current (DC) voltages of 0–1100 V were applied across the Ta probe and the nanorods.

C. Results and discussion

The FESEM images in Fig. 1 show the surface morphology of the niobium-oxide nanostructures. Fig. 1(a) displays a top view of the spectacular and scenic nanoscale farmland containing various

domains ranging in area from a few square submicrometers to a few square micrometers (see Supporting information, Fig. S1). Fig. 1(b) illustrates the top view of a portion of the scenic nanoscale farmland-like surface. It is clear that the various domains consist of varying niobium-oxide nanostructures. The high-magnification FESEM image in Fig. 1(c) shows a side view (70° to the surface normal direction) of a portion of a domain taken from the region highlighted by the white rectangular box in Fig. 1b. Obviously, the domain consists of vertically-aligned 1D niobium-oxide nanowires, which are, on average, ~ 20 nm wide. The tips of the 1D niobium-oxide nanorods are very sharp. The average diameter of the tips is ~ 2 nm wide. Each domain contains ~ 620 nanorods per square micrometer. The average length of the 1D niobium-oxide nanorods is ~ 230 nm, indicating the domain to be 230 nm higher than the neighbouring domain. Actually, the FESEM image in Fig. 1c does not show the real length of the 1D niobium-oxide nanorods, because only the top portions are seen, and the bottom portions are hidden. To find the real length, we must observe the scenic nanoscale farmland-like surface from the side (see Supporting information, Fig. S2). The FESEM image in Fig. 1(d) displays three other domains each possessing distinct niobium-oxide 1D nanorods with different growth directions (as indicated by the arrows), illustrating the multi-growth directions of the 1D niobium-oxide nanorods in the scenic nanoscale farmland-like surface. In addition, the XRD patterns (see Supporting information, Fig. S3) reveal the 1D niobium-oxide nanorods to be NbO_2 crystals only.

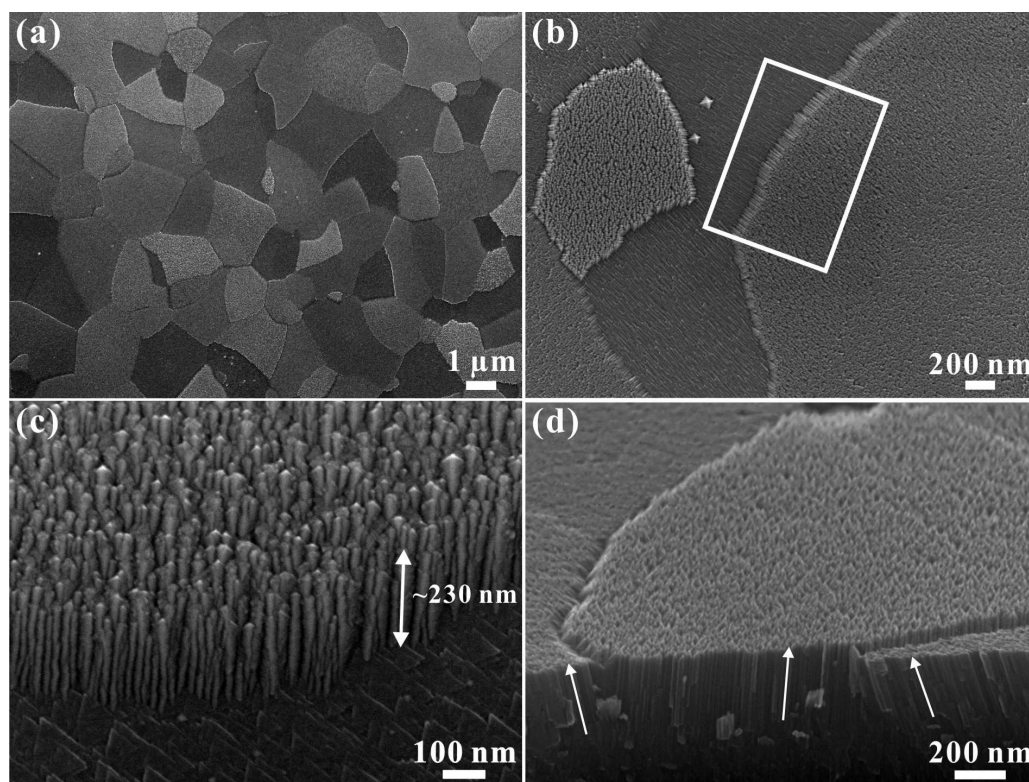


Fig. 1. FESEM images showing the surface morphology of the niobium-oxide nanostructures: (a) scenic nanoscale farmland-like surface containing various domains; (b) top view of a portion of the scenic nanoscale farmland-like surface with various domains consisting of varying niobium-oxide nanostructures; (c) side view (70° to the surface normal direction) of a portion of a domain taken from the region highlighted within a white rectangular box in (b). Each domain consists of vertically-aligned 1D niobium-oxide nanorods. (d) The other three domains possess niobium-oxide 1D nanorods with three distinct growth directions (indicated by the three arrows). The multi-growth directions of the 1D niobium-oxide nanorods give the sample appearance of scenic nanoscale farmland-like surface.

The bandgap and the trap levels are the two factors that give rise to PL emissions in undoped semiconducting materials. In semiconducting metal oxides, oxygen anions are easily volatilized to yield numerous oxygen vacancies.^[24,27] Oxygen vacancies are formed when oxygen anions escape from the surface. Each oxygen vacancy provides a reduction of two electrons at the two dangling bonds. The dangling bonds can give rise to the trap levels within the bandgap, which are able to trap excited electrons. When excited electrons drop from the trap levels (or conduction band) to the ground state (i.e., valence band), visible-light is emitted. Therefore, the presence of oxygen vacancies makes the metal oxides as *n*-type semiconductors, and plays a key role in the PL emissions. From this discussion, it can be concluded that the PL spectra are strongly affected by the bandgap and oxygen vacancies within the metal oxides. To determine the bandgap and trap levels of the 1D NbO₂ nanorods, the PL spectra are decomposed using Voigt function fitting. Fig. 2(a) shows the decomposed room-temperature PL spectra of the 1D NbO₂ nanorods with asymmetrical spectral features. Fitting of the asymmetrical emission peak is also accomplished using the Voigt function. After decomposition we find five peaks corresponding to the five light emissions of 443.0 (labeled a), 512.9 (labeled b), 556.6 (labeled c), 614.1 (labeled d) and 702.8 (labeled e) nm, with full widths at half-maxima (FWHM) of 89.4, 68.0, 89.3, 107.5 and 184.1 nm, respectively. Peak a apparently is

the main peak with the highest intensity in the PL spectra, so it represents the near band edge (NBE) electron transition. The NbO₂ nanorod bandgap is indicated to be 2.8 eV. The other small peaks (Peaks b-e) signify the intrinsic trap level electron transitions.^[24,27] Fig. 2(b) shows a schematic representation of the NBE and various trap level electron transitions. The b, c, d and e peaks correspond to the oxygen-vacancy trap levels of 2.42, 2.23, 2.02 and 1.76 eV, respectively. Electrons in the valence band are excited by an incident laser with a wavelength of 325 nm to a virtual state of 3.82 eV. The excited electrons likely to be trapped by the dangling bonds at the oxygen vacancies, make nonradiative transitions from the virtual state to the bottom of the conduction band, and then to the various trap levels. When the trapped electrons return to the valence band from the various trap levels, they emit photons (i.e., PL), releasing photonic energy via radiative transitions. The color space chromaticity diagram in Fig. 2(c) shows the color of the PL emissions from the 1D NbO₂ nanorods, obviously very purple-blue (as seen in the inset). This is because the PL emissions are mainly comprised of purple and blue light emissions, although the PL spectra in Fig. 2(a) consist of varying visible light emissions from purple to red. The 1D NbO₂ nanorods have effective purple-blue emissions at room temperature, so they are all potential candidates for use in optoelectronic nanodevices, such as light-emitting diodes and laser diodes in purple and blue.

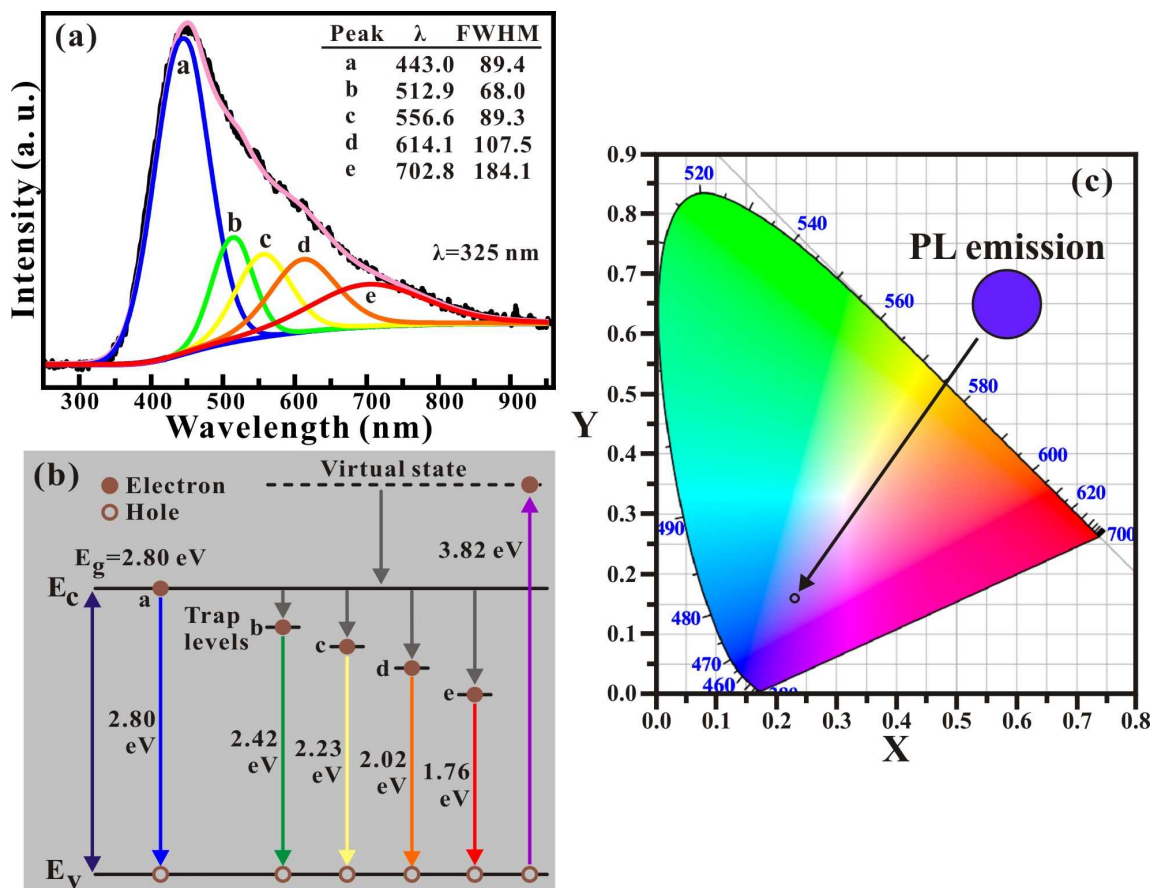


Fig. 2. (a) Decomposed room-temperature PL spectrum of the 1D NbO₂ nanorods. The PL spectrum is decomposed using Voigt function fitting. (b) Bandgap and trap-level emission energy diagram of the 1D NbO₂ nanorods. (c) Color space chromaticity diagram of PL emissions from the 1D NbO₂ nanorods. The inset to (c) shows that the PL emissions appear purple-blue.

COMMUNICATION

Field emission (FE) is a physical phenomenon where electrons are emitted into a vacuum from sharp-tip features at large negative applied voltages. The sharp-tip features can easily enhance the FE properties, because the negative applied voltages provide electrons at the top with sufficient energy to tunnel through the potential barrier between the sharp-tip features and metallic electrodes. Most 1D metal-oxide nanostructures have sharp-tip features at the ends. As shown in Fig. 1(c), the 1D NbO₂ nanorods have a sharp tip with a radius of curvature of ~1 nm, so they should be good electron emitters. The photographs in Fig. 3(a) illustrate the setup for FE measurement with a Ta ball-probe. The inset to Fig. 3(a) shows a Ta ball-probe with a radius ($\equiv r$) of ~750 μm , which can approach to about 50 μm ($\equiv d_1$) away from the 1D NbO₂ nanorods. Examination of the graph in Fig. 3(b) shows that the normalized applied field between the anodic ball-probe and the cathodic sample surface varies inversely with the ratios of d_2 to d_1 , where d_1 (=50 μm) and d_2 are the separation from the center and side, respectively, of the ball-probe to the surface (see the schematic diagram inset to Fig. 3(b)). The applied field is 100 % normalized, when the d_2/d_1 ratio is 1. The normalized applied field is inversely proportional to the d_2/d_1 ratio. When the d_2/d_1 ratio is 10, the normalized applied field is only 10 % (as indicated by the green dashed-line). Therefore, the effective area is determined using a d_2/d_1 ratio of 10 for the FE

measurements. The effective area contains the 1D NbO₂ nanorods that mainly contribute to the FEs. We can obtain an effective area of $A_{\text{eff}} = \pi r^2 \sin^2 \theta \approx 1.48 \times 10^6 \mu\text{m}^2$, where $r = 750 \mu\text{m}$ and $\theta \approx 66.42^\circ$. As mentioned above, each square micrometer contains ~620 nanorods. Altogether the A_{eff} contains $\sim 9.2 \times 10^8$ nanorods. As shown in Fig. 1(c), each nanorod with a tip radius ($\equiv r_{\text{tip}}$) of curvature of ~1 nm can provide a hemispherical area of $A_{\text{hemi}} = 2\pi r_{\text{tip}}^2 \approx 6.3 \times 10^{-6} \mu\text{m}^2$ for FE measurement, which gives us a total effective area of $A_{\text{tot}} = 9.2 \times 10^8 \times A_{\text{hemi}} = 5.8 \times 10^3 \mu\text{m}^2$. In addition, we need to determine the applied field between the ball-probe and the sample surface for FE measurement. Since the surface of the ball-probe is curved, not flat, it is important to ascertain the separation between the ball-probe and the sample surface for the applied field. Statistically, we employ the root-mean-square (RMS) method to obtain the RMS separation ($\equiv d_{\text{RMS}}$) to acquire the applied field. The RMS separation is defined as

$$d_{\text{RMS}} = \sqrt{\frac{\int_0^\theta (d_1 + r - r \cos \theta)^2 d\theta}{\theta}}, \quad (1)$$

so we can obtain $d_{\text{RMS}} = 247.9 \mu\text{m}$ and the RMS applied field is $E_{\text{RMS}} = V/d_{\text{RMS}}$. Therefore, the E_{RMS} can be used to represent the applied field between the ball-probe and the sample surface.

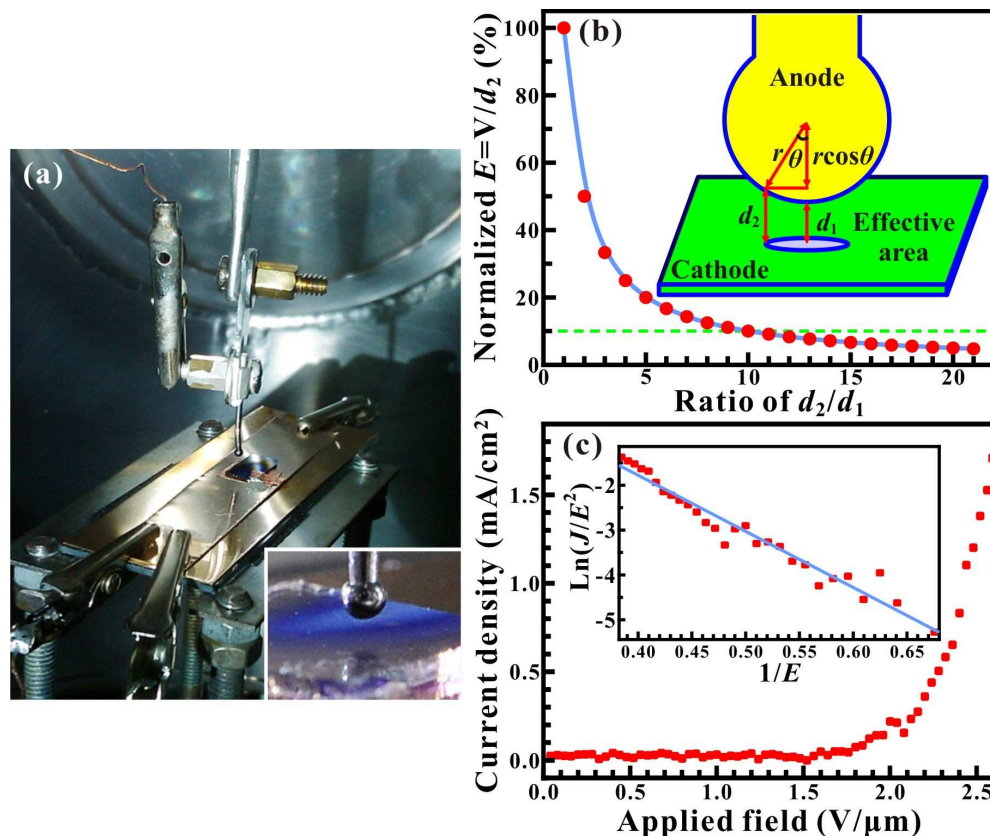


Fig. 3. (a) Photographs showing the setup for FE measurement with a Ta ball-probe: (b) graph of the normalized applied field E versus the ratio of d_2/d_1 between the ball-probe and the sample surface. The green dashed-line indicates 10 % E at $d_2/d_1 = 10$. The inset to (b) displays the geometry of the ball-probe and the separation from the sample surface. (c) FE J - E characteristics of the 1D NbO₂ nanorods. The inset to (c) shows the FN plot and slope for the field enhancement factor β .

The linear graph in Fig. 3(c) shows a typical FE current density (J) versus applied field (E) for the 1D NbO₂ nanorods. The good J - E characteristics of the 1D NbO₂ nanorods reveal very low turn-on and threshold fields of 1.5 and 2.4 V/ μ m, respectively, at current densities of 11.2 μ A/cm² and 1.1 mA/cm². The FE results are much smaller than those for the other metal-oxide nanostructures,^[5] indicating the 1D NbO₂ nanorods to be excellent electron emitters. Their FE properties can be further described by the Fowler-Nordheim (FN) equation,

$$J = (A\beta^2 E^2 / \varphi) \exp(-B\varphi^{3/2} / \beta E), \quad (2)$$

where J is the current density (mA/cm²), E is the applied field (V/ μ m), the universal constants are $A=1.54 \times 10^{-6}$ A eV V⁻² and $B=6.83 \times 10^3$ eV^{-3/2} Volt μ m⁻¹, β is the field-enhancement factor, and φ is the work function of the emitter. The work function (=5.6 eV) of Nb₂O₅^[5] is used for the FN equation to obtain the FN plot of $\ln(J/E^2)$ versus $1/E$, shown in the inset to Fig. 3(c). The slope of the FN plot represents the field enhancement factor β , which is found to be 7256. The large β represents a high field emitting efficiency, implying again that the 1D NbO₂ nanorods are excellent electron emitters and thus a promising candidate material for FE nanodevices, such as commercial flat displays.

Conclusions

We used the HFMOVD technique to synthesize a scenic nanoscale farmland-like surface of 1D NbO₂ nanorods arranged in the various domains. The 1D NbO₂ nanorods have multi-growth directions, with each domain having its own growth direction and containing ~620 nanorods. The room-temperature PL spectra show the 1D NbO₂ nanorods to provide intensive PL emissions from UV to IR at room temperature, while the PL emissions simultaneously emerging from the bandgap and numerous trap levels look purple-blue. The room-temperature FE graphs demonstrate that the 1D NbO₂ nanorods have very low turn-on (1.5 V/ μ m) and threshold (2.4 V/ μ m) fields and a large field enhancement factor ($\beta=7256$). Consequently, the effective FE characteristics confirm the possibility of using large-scale high-density 1D NbO₂ nanorod arrays as candidates for field electron emitters.

Acknowledgements

The authors would like to thank the National Science Council of the Republic of China for their financial support of this research under Contract Nos. NSC-101-2112-M-259-003-MY2, NSC-102-2923-M-259-001-MY3, NSC-102-2811-M-259-013, NSC-103-2112-M-259-006-MY2 and NSC-103-2811-M-259-003.

Notes and references

^a Department of Physics, National Dong Hwa University, Hualien 97401, Taiwan, Republic of China. Tel: +886-3-8633706; Fax: +886-3-8633690;

E-mail: ronma@mail.ndhu.edu.tw

^b Institute of Physics, Academia Sinica, Taipei 11529, Taiwan, Republic of China

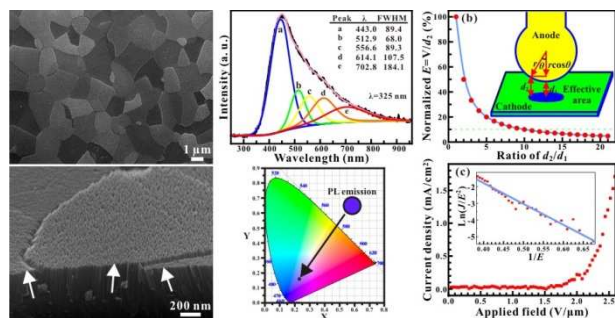
^c Department of Physics, University of Pune, Pune 411007, Maharashtra, India

^d Graduate Institute of Applied Science and Technology, National Taiwan University of Science and Technology, Taipei 106, Taiwan, Republic of China

- 1 R. S. Devan, R. A. Patil, J.-H. Lin, and Y.-R. Ma, *Adv. Funct. Mater.* 2012, **22**, 3326.
- 2 D. Bach, H. Stormer, R. Schneider, D. Gerthsen, and J. Verbeeck, *Microsc. Microanal.* 2006, **12**, 416.
- 3 Y. Zhao, Z. J. Zhang, and Y. H. Lin, *J. Phys. D-Appl. Phys.* 2004, **37**, 3392.
- 4 U. Cvelbar, and M. Mozetic, *J. Phys. D-Appl. Phys.* 2007, **40**, 2300.
- 5 B. Varghese, S. C. Haur, and C. T. Lim, *J. Phys. Chem. C* 2008, **112**, 10008.
- 6 M. D. Wei, Z. M. Qi, M. Ichihara, and H. S. Zhou, *Acta Mater.* 2008, **56**, 2488.
- 7 H. Y. Luo, M. D. Wei, and K. M. Wei, *J. Nanomater.* 2009, 758353.
- 8 H. Wen, Z. F. Liu, J. Wang, Q. B. Yang, Y. X. Li, and J. Yu, *Appl. Surf. Sci.* 2011, **257**, 10084.
- 9 M. J. Sayagues, and J. L. Hutchison, *J. Solid State Chem.* 2002, **163**, 137.
- 10 M. J. Sayagues, and J. L. Hutchison, *J. Solid State Chem.* 1996, **124**, 116.
- 11 M. J. Sayagues, and J. L. Hutchison, *J. Solid State Chem.* 1999, **146**, 202.
- 12 S. Venkataraj, R. Drese, C. Liesch, O. Kappertz, R. Jayavel, and M. Wuttig, *J. Appl. Phys.* 2002, **91**, 4863.
- 13 M. Vinnichenko, A. Rogozin, D. Grambole, F. Munnik, A. Kolitsch, W. Moller, O. Stenzel, S. Wilbrandt, A. Chuvilin, and U. Kaiser, *Appl. Phys. Lett.* 2009, **95**, 081904.
- 14 M. Mozetic, U. Cvelbar, M. K. Sunkara, and S. Vaddiraju, *Adv. Mater.* 2005, **17**, 2138.
- 15 J. H. Lim, and J. Choi, *J. Ind. Eng. Chem.* 2009, **15**, 860.
- 16 Y. Lin, Y. J. Yang, and C. C. Hsu, *Thin Solid Films* 2011, **519**, 3043.
- 17 Y. Kobayashi, H. Hata, M. Salama, and T. E. Mallouk, *Nano Lett.* 2007, **7**, 2142.
- 18 Y.-R. Ma, C.-M. Lin, C.-L. Yeh, and R.-T. Huang, *J. Vac. Sci. Technol. B* 2005, **23**, 2141.
- 19 Y.-R. Ma, C.-C. Tsai, S.-F. Lee, K.-W. Cheng, Y. Liou, and Y.-D. Yao, *J. Magn. Magn. Mater.* 2006, **304**, E13.
- 20 L. Kumari, Y.-R. Ma, C.-C. Tsai, Y.-W. Lin, S.-Y. Wu, K.-W. Cheng, and Y. Liou, *Nanotechnology* 2007, **18**, 115717.
- 21 L. Kumari, J.-H. Lin, and Y.-R. Ma, *J. Phys.-Condes. Matter* 2007, **19**, 406204.
- 22 L. Kumari, J.-H. Lin, and Y.-R. Ma, *Nanotechnology* 2007, **18**, 295605.
- 23 R. S. Devan, W.-D. Ho, J.-H. Lin, S.-Y. Wu, Y.-R. Ma, P.-C. Lee, and Y. Liou, *Cryst. Growth Des.* 2008, **8**, 4465.
- 24 R. S. Devan, W.-D. Ho, C.-H. Chen, H.-W. Shiu, C.-H. Ho, C.-L. Cheng, S.-Y. Wu, Y. Liou, and Y.-R. Ma, *Nanotechnology* 2009, **20**, 445708.
- 25 R. S. Devan, W.-D. Ho, S.-Y. Wu, and Y.-R. Ma, *J. Appl. Crystallogr.* 2010, **43**, 498.
- 26 R. S. Devan, J.-H. Lin, W.-D. Ho, S. Y. Wu, Y. Liou, and Y.-R. Ma, *J. Appl. Crystallogr.* 2010, **43**, 1062.
- 27 R. S. Devan, C.-L. Lin, S.-Y. Gao, C.-L. Cheng, Y. Liou, and Y.-R. Ma, *Phys. Chem. Chem. Phys.* 2011, **13**, 13441.
- 28 R. S. Devan, S.-Y. Gao, W.-D. Ho, J.-H. Lin, Y.-R. Ma, P. S. Patil, and Y. Liou, *Appl. Phys. Lett.* 2011, **98**, 133117.
- 29 R. A. Patil, R. S. Devan, J.-H. Lin, Y.-R. Ma, P. S. Patil, and Y. Liou, *Sol. Energy Mater. Sol. Cells* 2013, **112**, 91.

- 30 R. A. Patil, R. S. Devan, J.-H. Lin, Y. Liou, and Y.-R. Ma, *Sci. Rep.* 2013, **3**, 3070
- 31 L. Kumari, S.-J. Lin, J.-H. Lin, Y.-R. Ma, P.-C. Lee, and Y. Liou, *Appl. Surf. Sci.* 2007, **253**, 5931.
- 32 L. Kumari, J.-H. Lin, and Y.-R. Ma, *J. Phys. D-Appl. Phys.* 2008, **41**, 025405.
- 33 R. S. Devan, J.-H. Lin, Y.-J. Huang, C.-C. Yang, S. Y. Wu, Y. Liou, and Y.-R. Ma, *Nanoscale* 2011, **3**, 4339.
- 34 J.-H. Lin, Y.-J. Huang, Y.-P. Su, C.-A. Liu, R. S. Devan, C.-H. Ho, Y.-P. Wang, H.-W. Lee, C.-M. Chang, Y. Liou, and Y.-R. Ma, *RSC Adv.* 2012, **2**, 2123.

Table of Contents Entry



Nanoscale farmland-like surfaces of NbO₂ nanorods with multi-growth directions were synthesized, and the purple-blue photoluminescence and low-field emissions were shown.